FFI-rapport 2008/00847

Automatic ship detection based on satellite SAR

Camilla Brekke

Forsvarets forskningsinstitutt/Norwegian Defence Research Establishment (FFI)

4 May 2009

FFI-rapport 2008/00847

1104

P: ISBN 978-82-464-1582-6
E: ISBN 978-82-464-1583-3

Keywords

SAR

AIS

Automatisk skipsdeteksjon

Tersklingsalgoritmer

Approved by

Richard Olsen	Project manager
Johnny Bardal	Director

English summary

This report focuses on ship detection based on satellite Synthetic Aperture Radar (SAR) images. Imagery from the European ENVISAT satellite is analysed and Automatic Identification System (AIS) data from the Norwegian Coastal Administration (Kystverket) is applied for verification.

Aegir is a tool for analysis of SAR images developed at FFI. Aegir contains a module for ship detection. Two different thresholding algorithms for automatic ship detection, N-sigma and K-distribution, are implemented in Aegir. The algorithms are tested on ENVISAT ASAR Alternating Polarisation (AP) images. The results from these experiments are presented in this report.

The results show that the total number of alarms generated for co-polarised channels (VV and HH) is larger than the total number of alarms generated for cross-polarised channels (VH and HV). This result is independent of the choice of algorithm: N-sigma or K-distribution.

For the N-sigma algorithm, we found a higher false alarm rate for VV and HH than for VH and HV. A slightly higher number of verified ships were also detected in cross-polarisation.

Comparing the N-sigma algorithm with the K-distribution algorithm, we found that the K-distribution algorithm produces a lower false alarm rate both for cross-pol and co-pol data, compared to the N-sigma algorithm. However, slightly fewer verified ships were detected with the K-distribution algorithm compared to the N-sigma algorithm, both for cross-pol and co-pol.

In this context, it is important to remember that “false” alarms can be vessels without their AIS transponder turned on. In the case of a moving vessel, there could also be a time difference between the AIS reports and the SAR acquisition, making a match between the AIS position and the position in the SAR images highly uncertain. In addition, a ship which is heading in a non-azimuthal SAR direction will cause an azimuth displacement in the image, due to Doppler shift effects. This should also be taken into account when matching the SAR ship position with the positions found in the AIS reports [6] [12]. Further work should include a more detailed study of the causes of the false alarms. The algorithms should also be tested on a larger data material where scenes with varying sea state, incidence angle and polarisation are analysed.

The ship detection system described in this report is not yet mature enough for an operational context, and the results presented here must be viewed as preliminary. In the future, the K-distribution algorithm will be tested on coherence images (or Internal Hermittian Product (IHP) images) from Norut AS. The coherence images are generated based on single look complex data. The idea of such an approach is to utilize the higher phase coherence of a vessel than the surrounding sea to enhance the vessel signature and to suppress the sea surface signature [8]. The applicability of the K-distribution to model the sea clutter in these images still needs to be evaluated.

Sammendrag

Denne rapporten omhandler automatisk skipsdeteksjon basert på Syntetisk Apertur Radar (SAR)-bilder fra satellitt. Bildemateriale fra den europeiske ENVISAT satellitten er analysert. Data fra det norske Kystverkets Automatisk IdentifikasjonsSystem (AIS)-system er anvendt for verifikasjon.

Aegir er et verktøy for analyse av SAR-bilder utviklet ved FFI. Verktøyet inneholder en modul for skipsdeteksjon. To ulike tersklingsalgoritmer for automatisk skipsdeteksjon, kalt N-sigma og K-fordeling, er implementert i Aegir. Algoritmene er testet ut på ENVISAT ASAR Alternating Polarisation (AP) bilder. Resultater fra dette arbeidet er presentert i denne rapporten.

Resultatene viser at det totale antall alarmer generert for ko-polariserte kanaler (VV og HH) er større enn det totale antall alarmer generert for kryss-polariserte kanaler (VH og HV). Dette resultatet gjelder uavhengig av hvilken av de to algoritmene som kjøres.

For N-sigma algoritmen fant vi en høyere falsk alarm rate for VV og HH enn for VH og HV. Et noe høyere antall verifiserte skip ble også detektert i kryss-pol.

N-sigma algoritmen ble sammenliknet med K-fordelingsalgoritmen. Her fant vi at K-fordelingsalgoritmen produserer en lavere falsk alarmrate både for kryss-pol og ko-pol data sammenliknet med N-sigma, mens deteksjonsraten for verifiserte skip er noe lavere for K-fordelingsalgoritmen sammenliknet med N-sigma algoritmen, både for kryss-pol og ko-pol.

Det er viktig å huske i denne sammenhengen at “falske” alarmer kan være fartøy uten AIS-senderen skrudd på. Det kan også være en betydelig tidsforskjell mellom AIS rapportene fra det aktuelle fartøyet og SAR opptaket, som gjør at AIS posisjonen og posisjonen i SAR bildet ikke stemmer. Doppler skift, som fører til en forflytning av skipet i SAR bildet, er også en faktor det bør tas hensyn til når en skal fusjonere SAR posisjoner og AIS posisjoner [6][12]. Videre arbeid bør omfatte en mer detaljert studie av årsakene til de falske alarmene. Algoritmene bør også testes ut på et enda større datamateriale, hvor det legges vekt på analyse av scener med varierende sjøtilstand, innfallsvinkel, polarisasjon etc.

Det er viktig å understreke at skipsdeteksjonssystemet beskrevet i denne rapporten ikke er ferdig utviklet og testet og derfor heller ikke klar for operasjonell drift. I framtiden er det ønskelig å teste dette på koherensbilder (eller Internal Hermittian Product (IHP) bilder) fra Norut AS. Koherensbildene er generert basert på komplekse radarprodukter. Tanken er å forsterke signaturen til fartøyene samt å undertrykke støyen fra sjøen ved å utnytte at et fartøy har høyere koherens med hensyn på fasen enn den omliggende sjøen [8]. Hvor egnet K-fordelingen er til å modellere sjøstøyen i disse bildene gjenstår å vurdere.

Contents

Preface

This report is written in the context of project 1104 INNOSAT-II at FFI. INNOSAT-II focuses on satellite sensors and building up knowledge about space based surveillance of relevance for the Norwegian defence.

One of the project goals is to demonstrate and gain experience from the use of satellite SAR sensors. Within this context, we are also developing tools for analysis of satellite SAR images for maritime surveillance. The focus of this report is on automatic analysis of SAR images for ship detection.

We also have a collaboration with the EU project Land and Sea Integrated Monitoring for Environment and Security (LIMES) on this work (WP 5240 *Fusing polarimetric channels for SAR ship detection*). This report also addresses results for that work package.

1 Introduction

Synthetic Aperture Radar (SAR) data for ship detection are used today in operational maritime surveillance services in several countries and the European Union. However, further research is still needed to be able to fully exploit the information available from current and future SAR missions. The main goal of the present study is to develop an automatic algorithm for ship detection and type classification that takes advantage of new multi-polarised SAR products.

Eldhuset [7] demonstrated in a paper that automatic ship and ship wake detection methods work well both in Seasat and ERS-1 images. FFI is currently developing algorithms further, based on dual-polarised ENVISAT Advanced SAR (ASAR) data. Two thresholding algorithms are so far implemented for ship detection. Both algorithms are adaptive with respect to the image statistics.

In 2000-2004 [1], the International Maritime Organization (IMO) introduced regulations for the Automatic Identification System (AIS), requiring all major vessels to carry and operate a radio transponder capable of broadcasting and receiving identity and navigation information. Since 1st of January 2005, all vessels over 300 gross tons are required to operate an AIS transponder. While the AIS system was primarily intended to reduce collision risks at sea, many coastal nations, including Norway, have deployed networks of coastal AIS stations to enhance traffic monitoring in coastal waters. Norway is also developing a satellite mission with an AIS receiver payload, so that ship traffic can be monitored at sea in the High North. It will then be possible to fuse the information from satellite SAR with the information from satellite AIS. This will give us the possibility to identify detected ships within a SAR image.

In the mean time, information from ground-based coastal AIS systems can be used. From a SAR ship detection research point of view, AIS data contain very interesting parameters on ship size and type, as well as speed and heading. Fusion of AIS and SAR-derived parameters will enable us to develop further knowledge about SAR backscatter properties from different vessel types. In an operational context, it will also be possible to pin-point those ship candidates that do not carry an AIS system, and thereby let the responsible authorities take the appropriate actions.

In this report, we have fused SAR data and AIS data mainly for the purpose of validating the algorithms for automatic ship detection. This report summarizes results so far.

Ship detection based on current and future SAR missions are discussed in Chapter 0. The algorithms are described in Chapter 3, and the experimental results are presented in Chapter 4. A summary and thoughts about future work can be found in Chapter 5.

2 Ship Detection in Multi Polarimetric and High Resolution SAR Imagery

Dual-polarisation satellite SAR products (e.g. ENVISAT ASAR Alternating Polarisation (AP) mode) enable us to use two channels in automatic ship detection algorithms. In the future, we will

also get access to fully polarimetric SAR data (e.g. the Canadian RADARSAT-2 and the German TerraSAR-X satellites). Multi-polarised SAR data can lead to a more robust and accurate detection of ships. In addition, the possibilities for ship type classification should be explored when fully-polarised high resolution SAR data becomes available.

According to Arnesen and Olsen [2], analysis on ENVISAT ASAR AP images shows that the ship detection capability is improved with cross-polarised data for steep incidence angles. The Target-to-Clutter Ratio (TCR) is better for VH[1] and HV than for VV and HH for steep incidence angles (ASAR beams IS1-IS2, see Table 2). As a rule of thumb, the TCR should be at least 10 dB or better for automatic ship detection. Whereas co-polarised data (HH or VV) does not generally satisfy this criterion for IS1 (except in completely calm conditions), the cross-polarised data does. The situation is the opposite for shallow incidence angles, while the situation is not that clear at intermediary incidence angles. According to Attema [5] , there are indications that ship detection is best using HH polarised data for incidence angles > 45 degrees and using cross polarised data for incidence angles < 45 degrees.

Here, we have also looked at some ship length estimates based on ENVISAT ASAR AP data (IS6 and IS4). Figure 2.1 shows photos of the two vessels Baltica Hav and Bourbon Mistral. Their AIS-positions match the positions of the detections in Figure 2.2 and Figure 2.3.

Figure 2.4 and Figure 2.5 show a couple of more examples.

Figure 2.1 Left: Baltica hav. Length: 82.0 m Width: 11.0 m © Berge og Vegstein Skipsfoto. Right: Bourbon Mistral. Length: 89.0 m Width: 20.0 m © Terje Moen

[1] VH: Vertically polarised transmitted. Horizontally polarised received.
HV: Horizontally polarised transmitted. Vertically polarised received.
HH: Horizontally polarised transmitted. Horizontally polarised received.
VV: Vertically polarised transmitted. Vertically polarised received.

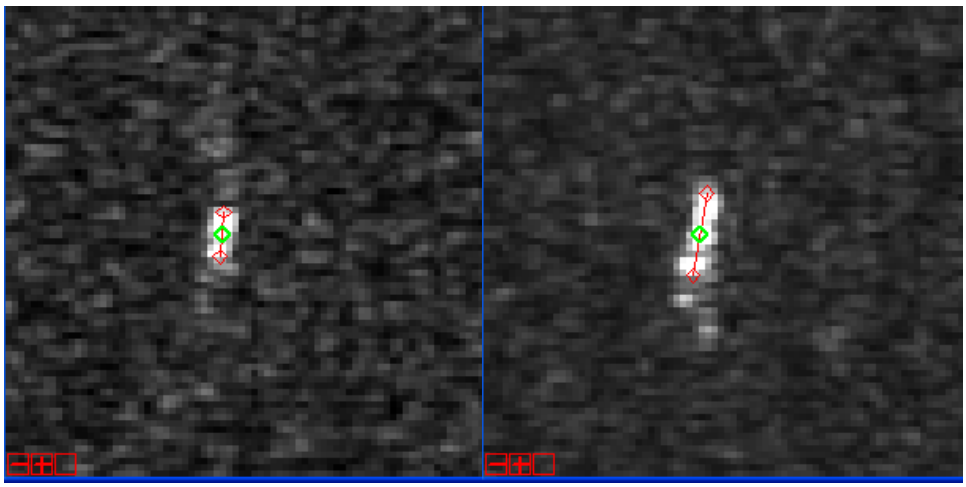

Figure 2.2 Baltica Hav. Reported by AIS: length: 82.0 m and width: 11.0 m. Left: HV, measured length 87.7 m. Right: HH, measured length 164.9 m. ENVISAT APP IS6 2007-10-26 T20:31:55

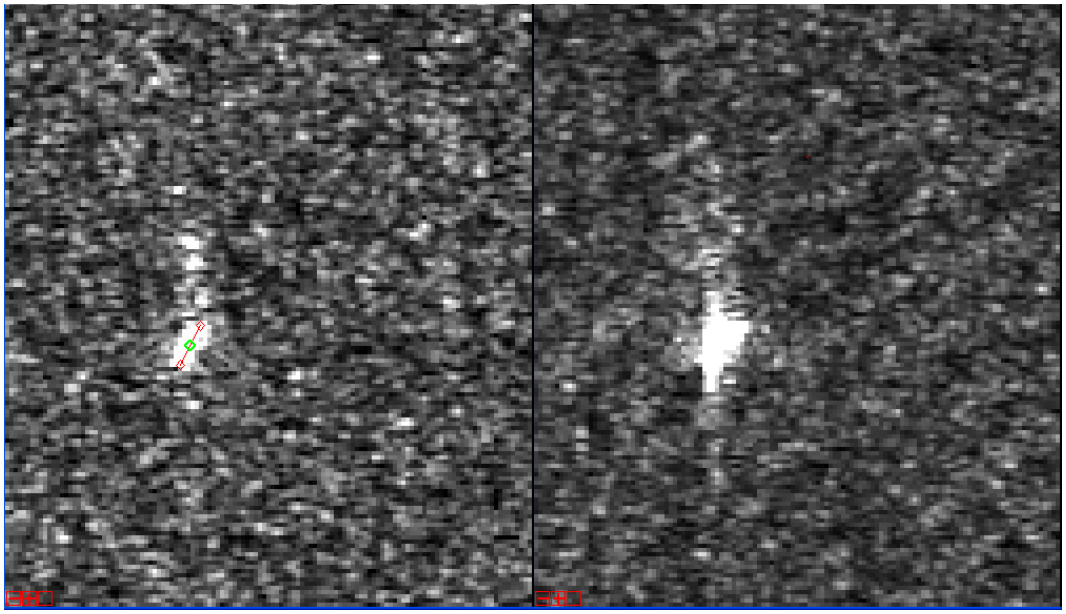

Figure 2.3 Bourbon Mistral. Reported by AIS: length: 89.0 m and width: 20.0 m. Left: VH, measured length: 132.8 m. Right: VV, not possible to measure length and orientation. ENVISAT APP IS4 19-NOV-2007 21:15:26.913348.

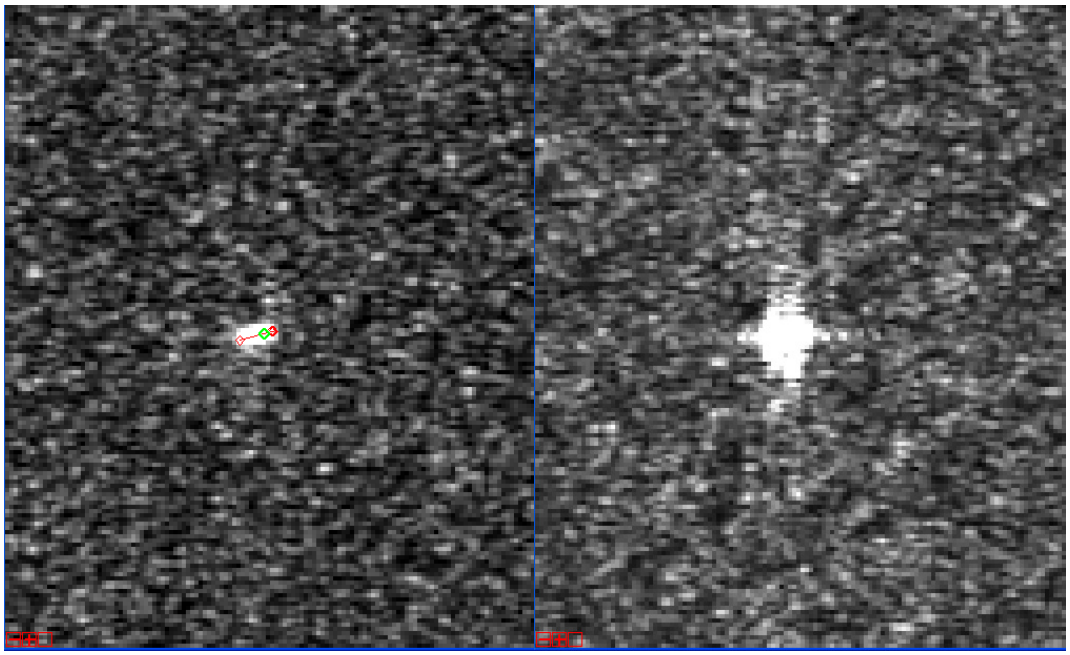

Figure 2.4 Cso Wellservicer. Reported by AIS:length: 103.0 m and width: 21.0 m. Left: VH, measured length: 103.3 m. Right: VV, not possible to measure length and orientation. ENVISAT APP IS4 19-NOV-2007 21:15:26.913348.

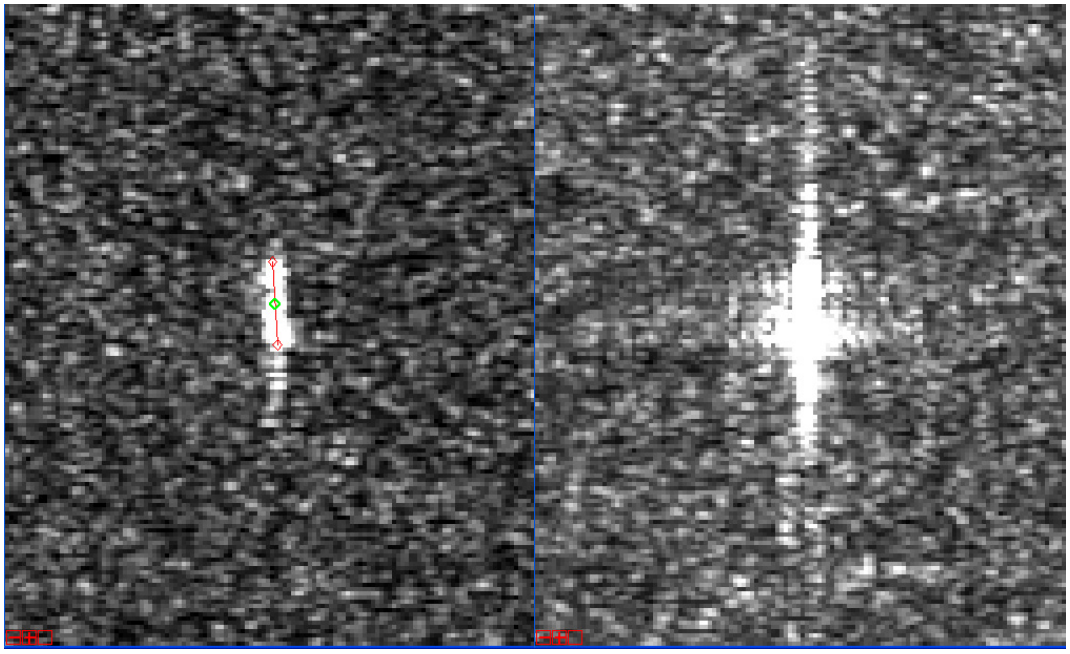

Figure 2.5 Bit Viking. Reported by AIS: length: 177.0 m and width: 26.0 m. Left: VH, measured length: 247.4 m. Right: VV, not possible to measure length and orientation. ENVISAT APP IS4 19-NOV-2007 21:15:26.913348.

In all these cases, the ship length measurements in the cross-polarised bands are more accurate than the ship length measurements in the co-polarised bands. In the co-polarisation cases from IS4, the orientation of the ships was also ambiguous, and therefore it was also not possible to estimate the ship length in Figure 2.3 to Figure 2.5.

Figure 2.6 shows an example of a SAR image acquisition from the TerraSAR-X satellite. The scene is from the Straight of Gibraltar. Several vessels are visible in the image. Figure 2.7 is zoomed in on a couple of the vessels. Many details are clearly visible. Unfortunately, we do not have access to AIS information matching this scene. However, fully polarimetric and high resolution data might have expanded potential for target detection, classification and orientation estimates compared to the SAR-products available from e.g. ENVISAT and RADARSAT-1.

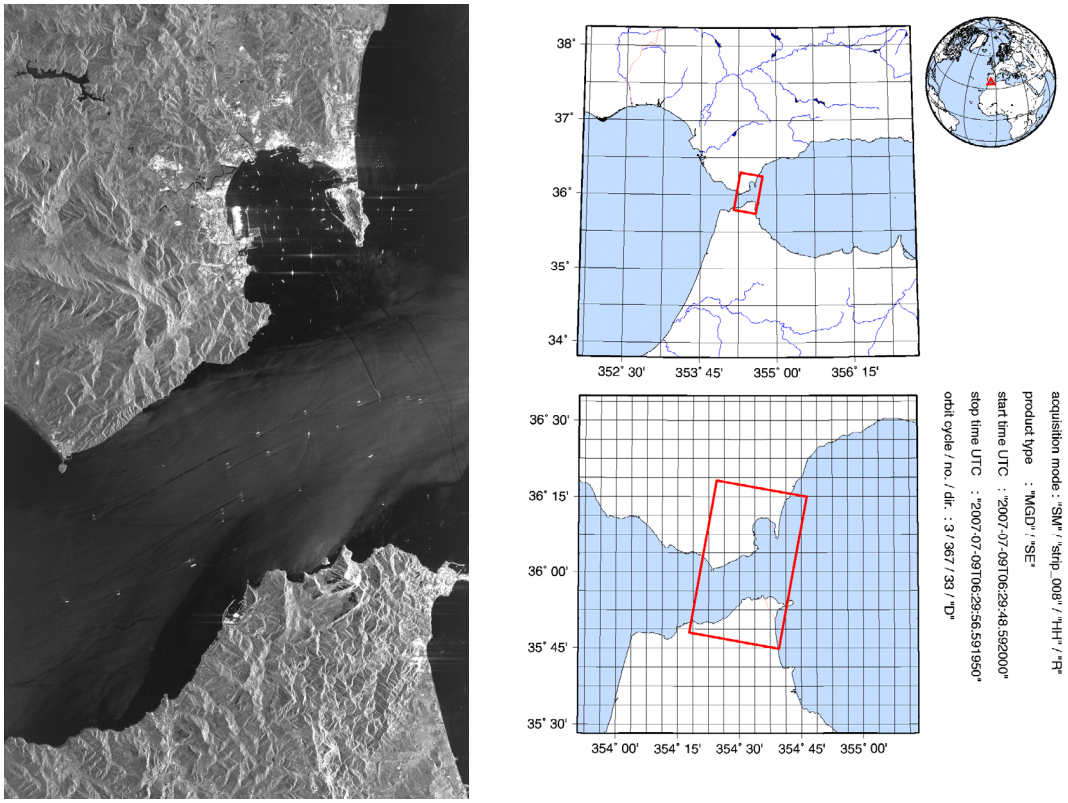

Figure 2.6 TerraSAR-X image, stripmap, 3 m resolution. Straight of Gibraltar. Many vessels are visible. © DLR (2007).

3 Automatic Ship Detection Algorithms

3.1 Methodology

The automatic algorithms for ship detection presented in this report are based on dual-polarised satellite SAR images. The automatic algorithms are implemented in an analysis tool named Aegir developed at FFI. See Figure 3.1 for an example of the Graphical User Interface. The framework of the automatic algorithms consists of the following elements:

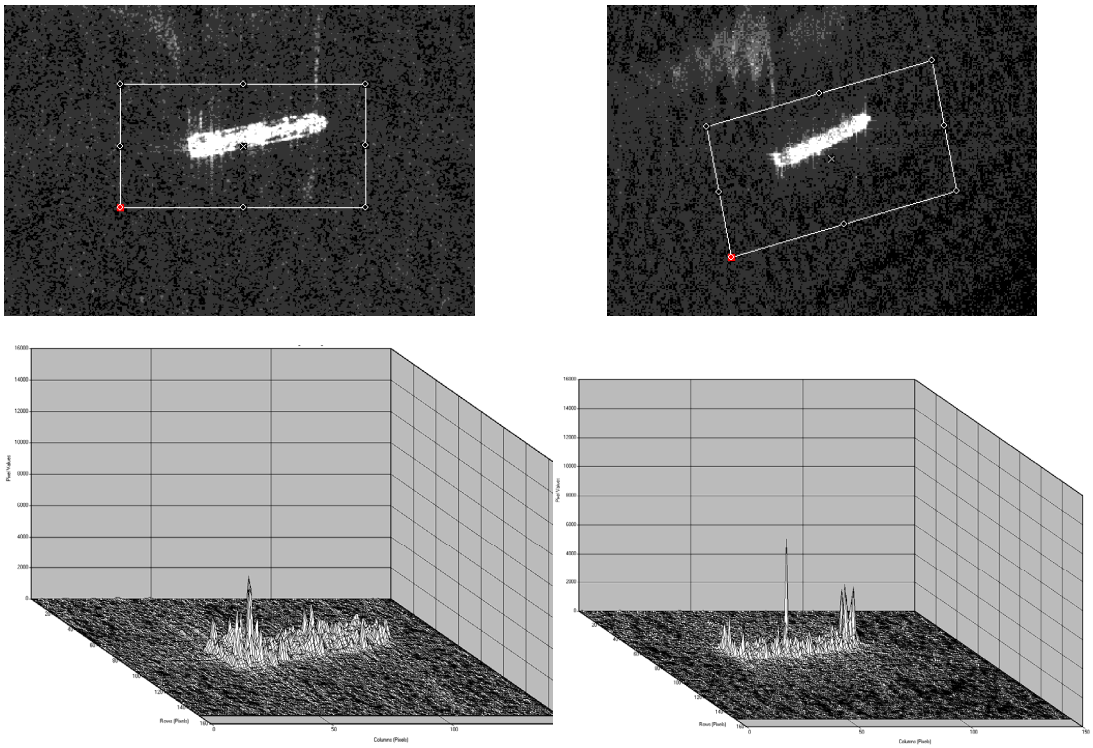

Figure 2.7 Zoom-in on a couple of the vessels visible in Figure 2.6 and their 3D signatures.

- A land/coastal mask to avoid searching for ships on land and to avoid mixing ships with smaller islands.
- Detecting bright targets sequentially in all available bands (e.g. for ENVISAT AP mode we have the combinations VV and VH or HH and HV or HH and VV).
- Estimate the detection confidence based on the combined results from the various bands.
- A manual verification step (see Figure 3.2 and Figure 3.3).

An additional step one could think of implementing in the future is:

- Ship type classification based on dimensions and backscatter signatures.

3.2 N-sigma Algorithm

The N-sigma algorithm is a very simple method for ship detection. In this algorithm, each band is first divided into frames of size M x M. The standard deviation and the mean value (σ, μ) are extracted from each frame *f*. For each individual frame, the threshold is set to *N* standard deviations above the mean value. See equation (3.1)

$$T_f = \mu_f + N * \sigma_f \tag{3.1}$$

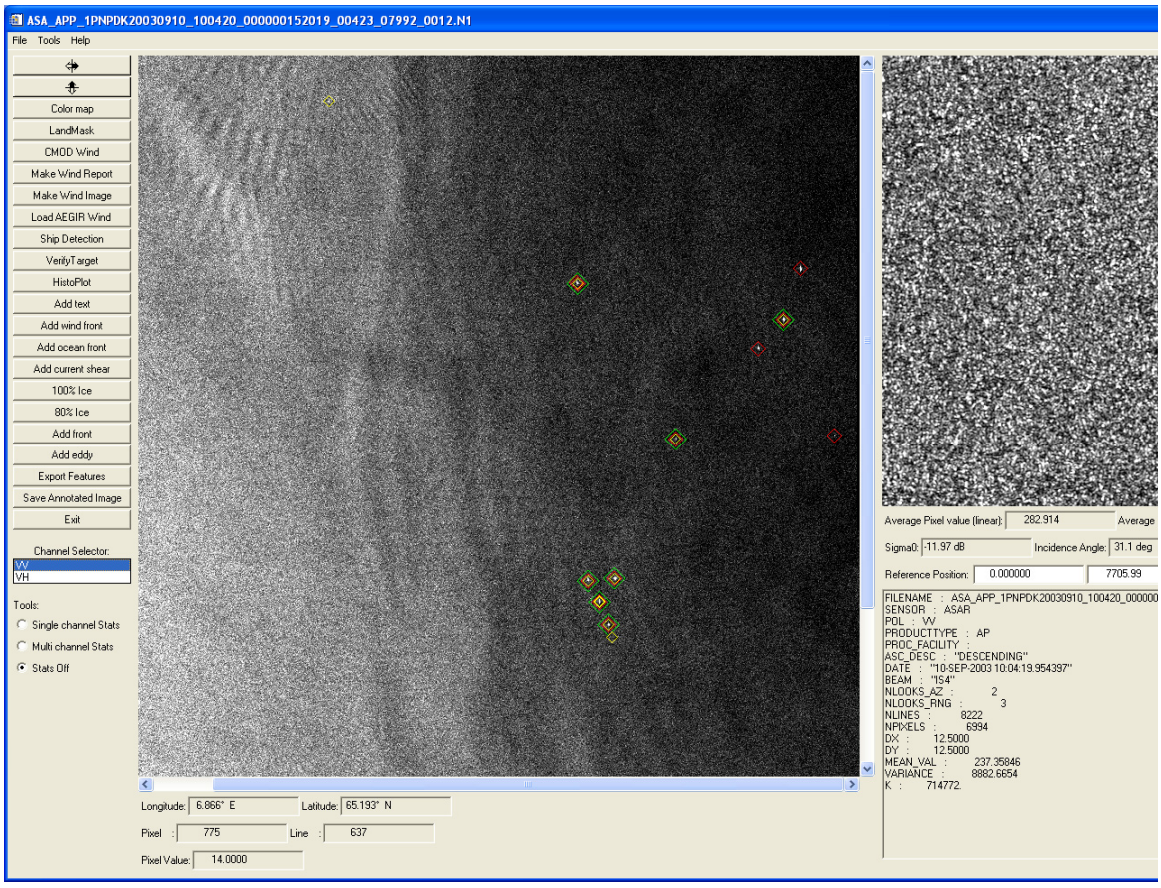

Figure 3.1 The "Ship detection" GUI of Aegir. The red and yellow squares are targets (ships, oilrigs) detected. In this case red are targets detected in VV while yellow are targets detected in VH. Green squares indicate targets detected in more than one band.

3.3 K-distribution Algorithm

A more sophisticated method is the K-distribution algorithm. In the K-distribution algorithm, each band is first divided into frames of size M x M. Like for the N-sigma algorithm, a threshold value is then estimated within each frame. However, in this case, a Probability Density Function (PDF) is adapted to the data, and then the threshold is estimated based on the PDF.

There are three main parameters involved in the K-distribution algorithm:

- *L* the Equivalent Number of Looks (ENL)[2] (estimated from image data)

[2] ENL: refers to groups of signal samples in a SAR processor that splits the full synthetic aperture into several sub-apertures, each representing an independent look of the identical scene. The resulting image formed by incoherent summing of these looks is characterized by reduced speckle and degraded spatial resolution [13].

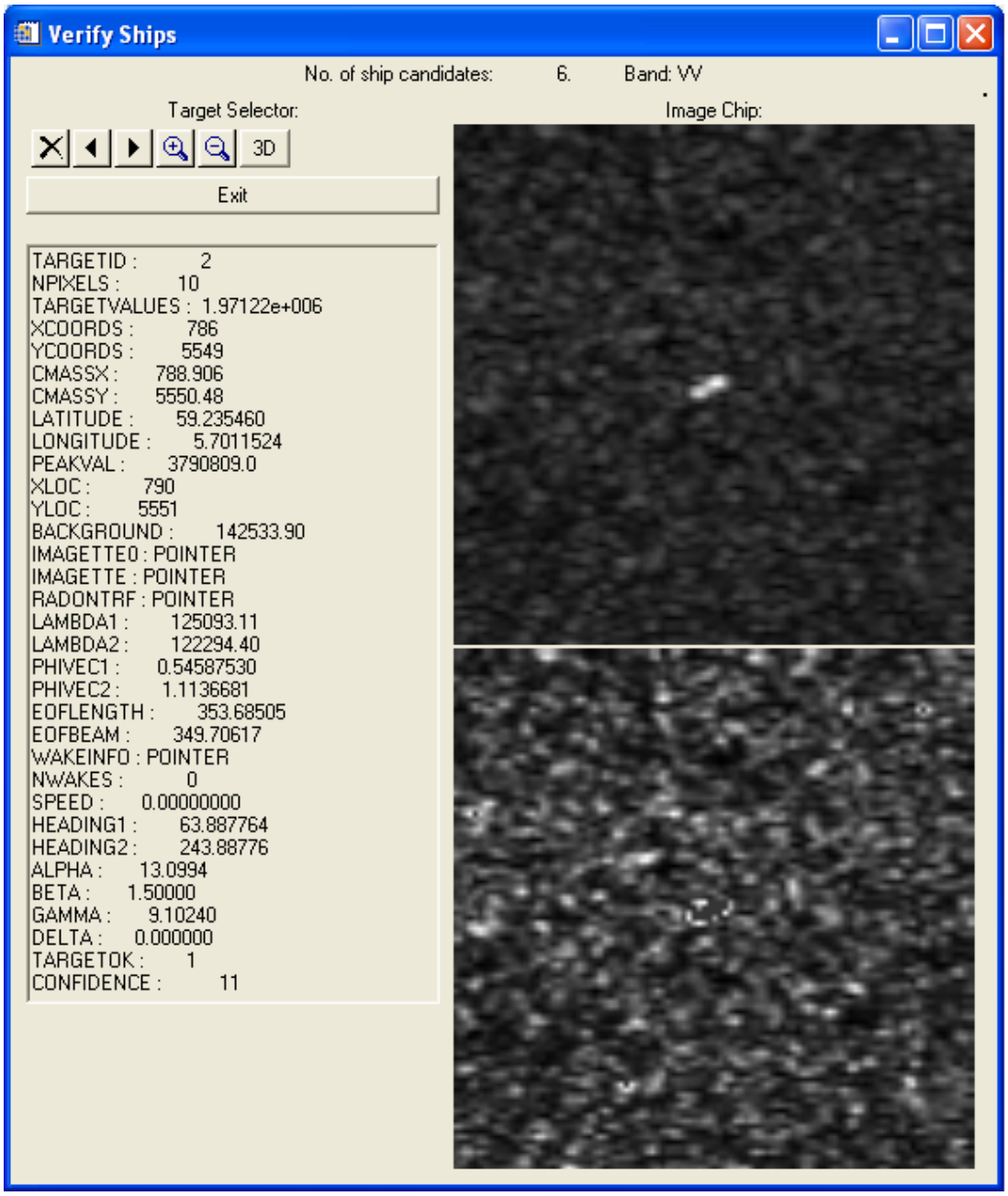

Figure 3.2 GUI of the "Verify ship" tool. The tool can be applied by the user to verify the vessels detected by the automatic algorithm. At the top of the GUI the label "Band: VV" indicates that these are ships detected in the VV channel. Comparable GUI's are available for all bands.

- v the order parameter of the K-distribution (estimated from image data)
- *CFAR* (Constant False Alarm Rate) (user specified)

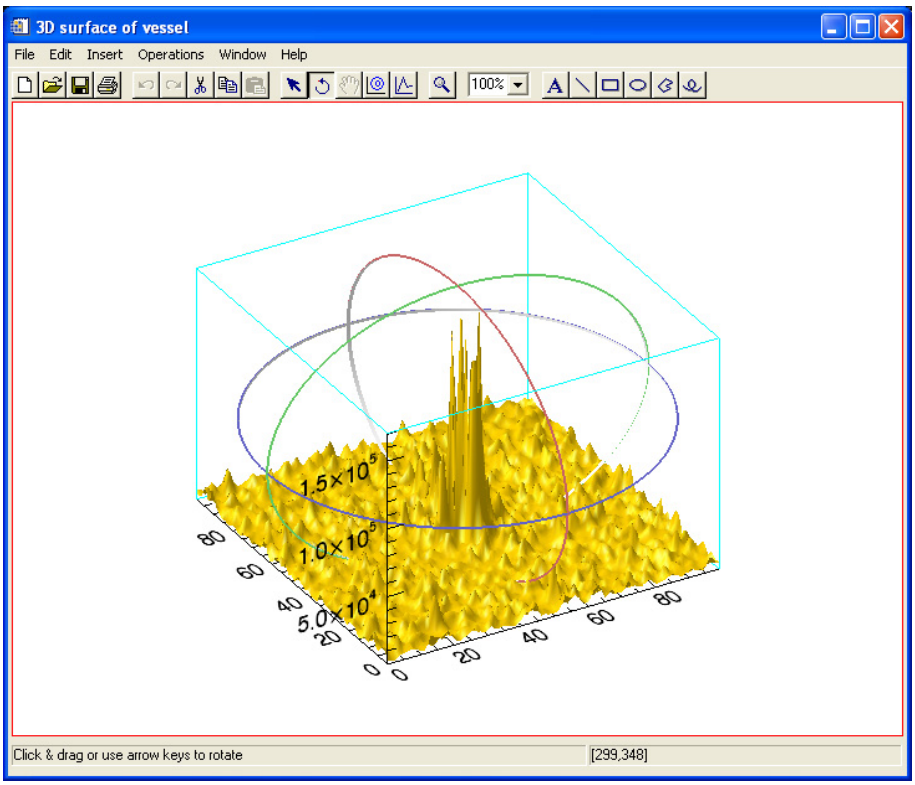

Figure 3.3 3D surface of a detected vessel. By pushing the "3D" button in the "Verify ship" tool this GUI becomes available. Here the user can view the detection from various angles and perform different operations on the plot (e.g filtering).

In order to be able to carry out CFAR detection of ships in SAR images, it is necessary to have a statistical model for the sea surface backscatter. In the radar field, the K-distribution is used extensively to represent sea clutter [9]. The K-distribution is a model for the statistics of SAR imagery that is formed from the product of two independent distributions, one representing the radar cross-section, and the other representing speckle that is a characteristic of coherent imaging [10]. Equation (3.2) represents the K-distribution.

$$p(x) = \frac{2}{x\Gamma(L)\Gamma(v)}\left(\frac{Lvx}{\mu}\right)^{\frac{(L+v)}{2}} K_{L-v}\left[2\sqrt{\frac{vLx}{\mu}}\right] \tag{3.2}$$

In equation (3.2), K is a modified Bessel function of order L-v. $p(x)$ is the PDF for the image intensity x. Γ is the gamma function. μ is the mean of the PDF and v is the order parameter of the intensity PDF that defines the skewness and the shape of the tail. Thus, it is important to obtain a good estimate for v to be able to set a proper threshold. Above this threshold, detected pixels will be expected to belong to a different population with a given probability [3]. L is the number of looks for the SAR image.

The theoretical K-distribution for some examples of different v values are shown in Figure 3.4.

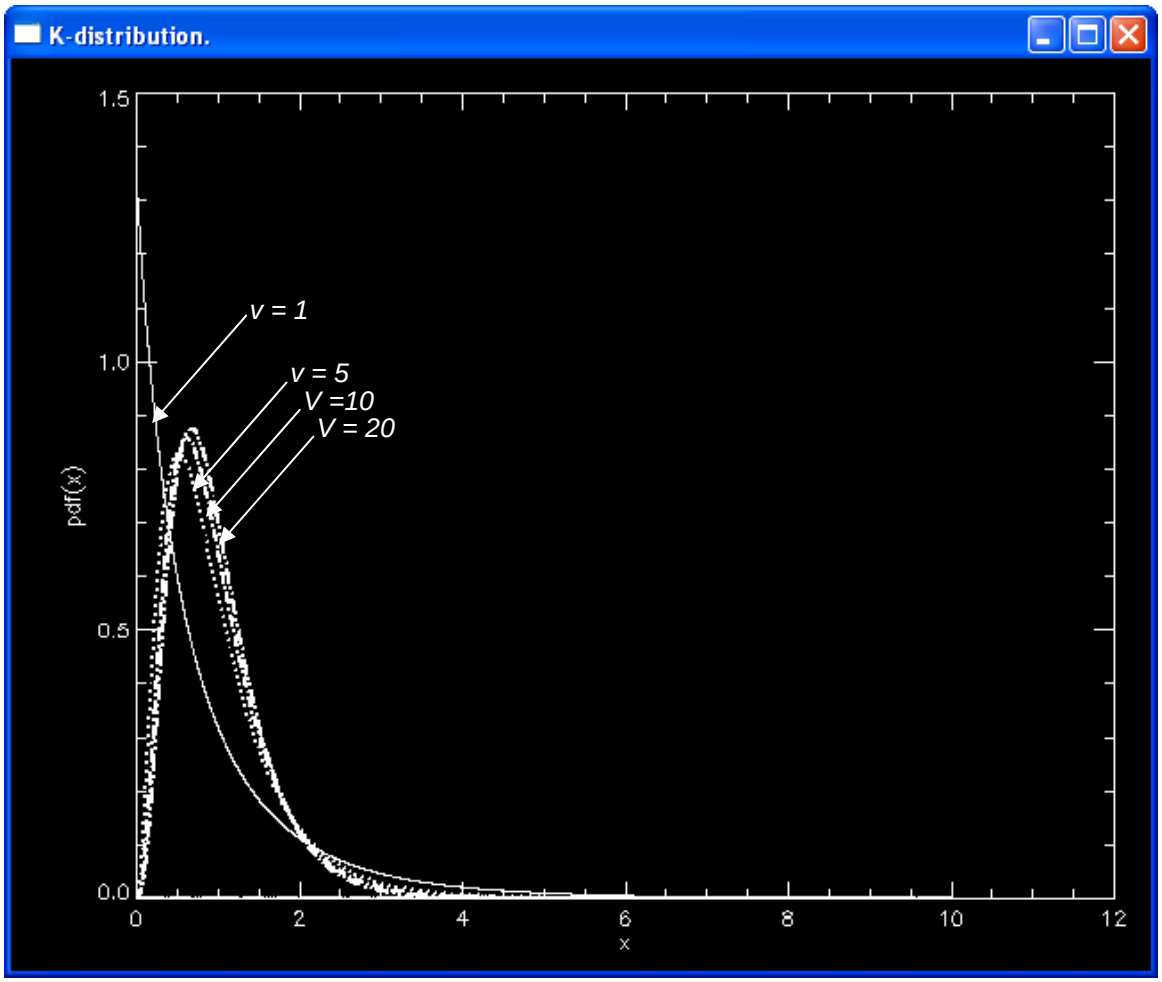

Figure 3.4 K-distribution for some values of the order parameter v. N=4 in this case and μ = 1

As the image pixels are represented as intensity values in our case, *ENL* is estimated according to equation (3.3) (for intensity/power data). In the algorithm, a final estimate of *ENL* is made for the whole image based on an average of ENL values from a selected number of frames within the image. The estimate of the ENL may be contaminated by high values from targets that are present. In order to avoid this, the highest 1% of the pixels within each frame is discarded before estimating the parameters.

$$ENL = \left(\frac{\mu}{\sigma}\right)^2 \tag{3.3}$$

We have implemented two different formulas for the estimation of the order parameter *v*. Estimates of the order parameter using the 1st approach of Blacknell [11] can be obtained by equation (3.4). Two other approaches by Blacknell are also described in [11]. Future work should include implementation and experimentation with these.

$$(1+\frac{1}{\hat{v}})(1+\frac{1}{L}) = \frac{\frac{1}{M}\sum_{i=1}^{M} x_i^2}{\left(\frac{1}{M}\sum_{i=1}^{M} x_i\right)^2} \tag{3.4}$$

The second approach is based on equation (3.5). Equation (3.5) was used to estimate the order parameter for the production of the results from the K-distribution algorithm presented in chapter 4. Equivalent experiments based on equation (3.4) should be done in the future.

$$\hat{v} = \frac{ENL+1}{ENL*\beta-1}, \beta = \frac{\sigma}{\mu^2} \tag{3.5}$$

Figure 3.5 illustrates the different results produced by equation (3.4) (Method 1) and equation (3.5) (Method 2) for the estimation of the order parameter *v*. For the VV channel, both Method 1 and Method 2 give an increase in the estimated order parameter for frames in the outer swath (large frame numbers in Figure 3.5). This is not the case for the VH channel. For Method 2, we can see a large variation in the estimated order parameters for the VH channel. We also got some negative estimates for a few of the frames in the VH channel when applying Method 2. The estimates from these frames are not plotted in Figure 3.5.

Figure 3.6 and Figure 3.7 show examples of the distribution of intensity values and the theoretical PDFs.

CFAR is the probability of a false alarm in a background region, and the threshold is set to yield a certain user selected CFAR. See equation (3.6).

$$CFAR = 1 - \int_0^{I_T} p(x)dx \tag{3.6}$$

In this study, for a given *v*, *ENL* and CFAR, *t* is looked up from the tables presented in Appendix A. After *t* is retrieved, the threshold within a particular frame f is set according $t\mu_f$. For fast processing, we have created two look-up-tables for *t* (see Appendix A). One table is generated for CFAR = 10^{-7} and the other one for CFAR=10^{-8}.

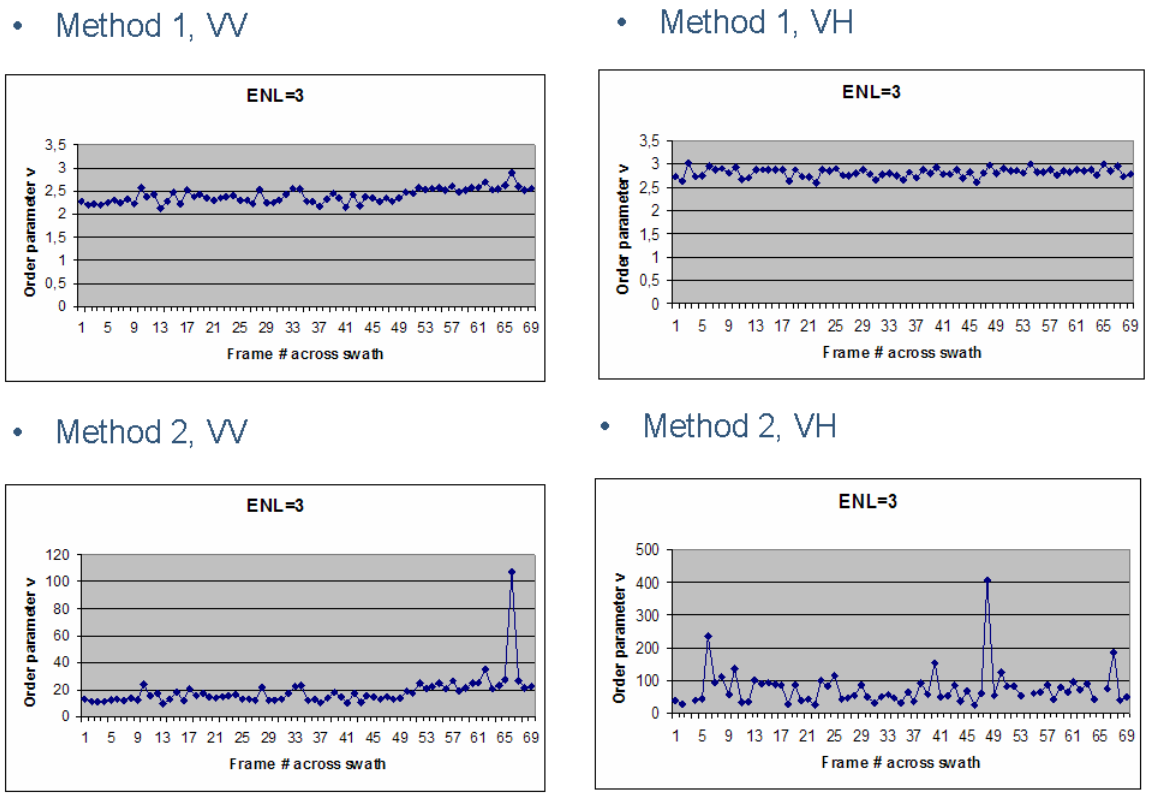

Figure 3.5 Estimates of the order parameter for various frames across the swath (a frame size of 100 x 100 pixels is applied) of an ENVISAT AP image from 10th September 2003. Method 1: Blacknell's first approach for order parameter estimation, equation (3.4). Method 2: Estimates of the order parameter based on equation (3.5).

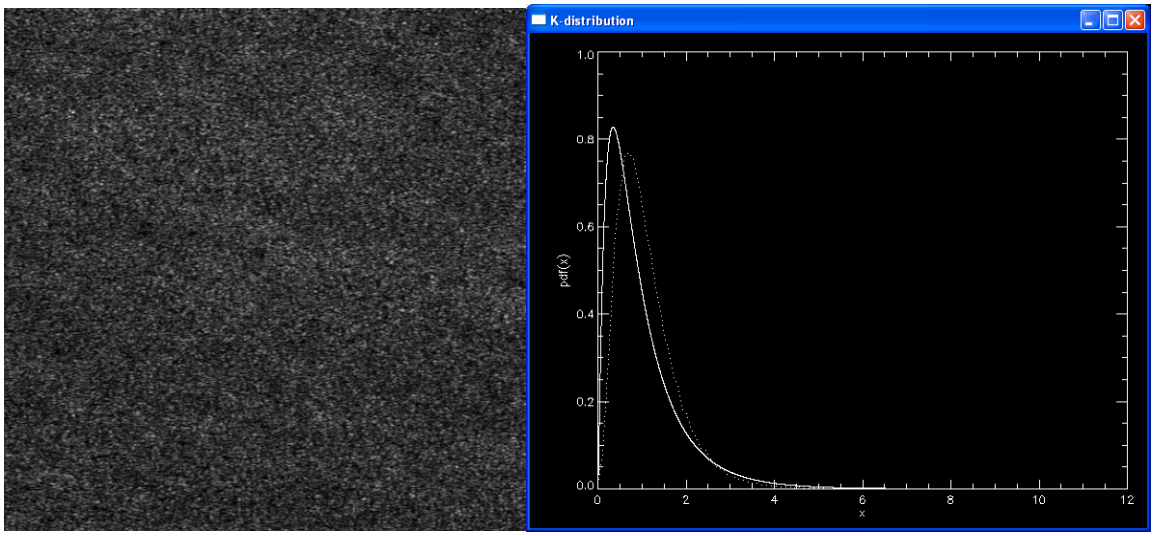

Figure 3.6 Left: subscene (500 x 500 pixels) of image 20071106 VH/VV IS7 (VV applied). Sea surface. Right: scaled values for the sea surface intensity values (dotted line), theoretical PDF (solid line). Estimated v: 3.

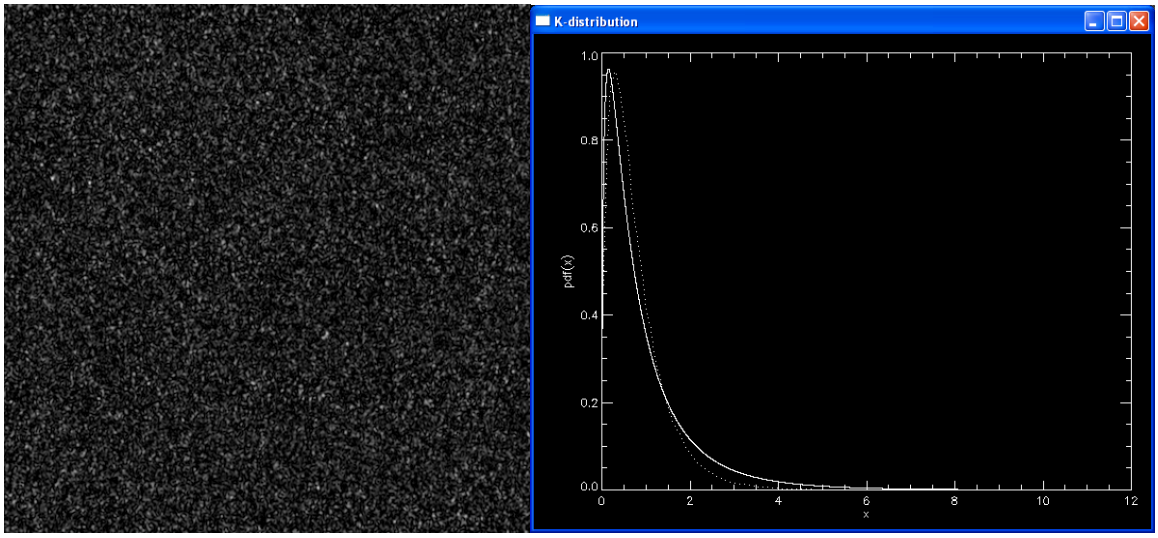

Figure 3.7 Left: subscene (500 x 500 pixels) AP 20050225 IS1 HV/HH (HH applied). Sea surface. Right: scaled values for the sea surface intensity values (dotted line), theoretical PDF (solid line). Estimated v: 2.

3.4 Result Reports

A list of detected targets is produced as an output form the ship detector. The list contains the following attributes:

- Polarisation (VV, HH, HV or VH)
- Size (number of pixels)
- Peak value
- Target position (CmassX, CmassY, longitude, latitude)
- Estimated ship length (LOA)
- Estimated ship beam
- Estimated heading (estimate 1)
- Estimated heading (estimate 2)
- Detection confidence

In addition, the detected targets are plotted as symbols overlaid the SAR image. An example was given in Figure 3.1.

Table 3.1 gives an example of a report produced by the ship detector. In this case it is an AP (HH/HV) image that is processed. The results from the various polarisation bands are merged in this report. Corresponding detections in the other band are presented in "()".
In this case, detections with confidence above 500 are detected in both bands. This is a user specified value (see Figure 3.8). To locate dual detections we have used the target position; specifically the centre of mass. If the x, y coordinates of the centre of mass of two detections in separate bands are located within +- 10 pixels of each other, the estimated detection confidences (*CE*) are increased with the user specified value *e* according to equation (3.7).

$$CE' = CE + e \tag{3.7}$$

Kongsberg Satellite Services (KSAT) has defined a standard ship detection report which is used as part of a service for the European Maritime Safety Agency (EMSA) and for the Land and Sea Integrated Monitoring for Environment and Security (LIMES) project (see Appendix C). We should probably adapt to this in the future.

```
Sensor: ASAR       Date: "31-JAN-2008 21:21:14.528510"
Pol.    No. of Pixels  Peak Val      CmassX        CmassY        Longitude      Latitude
LOA             Beam             Hdg1           Hdg2         Confidence
================================================================================================
================================================================================
HH (HV)           6 (6)       37576900. (1234321.0)      3352.09 (3352.54)      501.579
(500.283)       5.8807230 (5.8808561)       59.047157 (59.047055)       11.691781
(11.322833)       6.2188210 (10.601923)       86.389323 (13.083247)       266.38932
(193.08325)         505 (503)

HH (HV)          11 (6)       4950625.0 (478864.00)      1696.81 (1695.87)      673.578
(673.468)       5.5190310 (5.5188294)       59.034489 (59.034471)       23.100642
(14.647410)       8.1645120 (9.3309072)       80.942801 (28.613513)       260.94280
(208.61351)         514 (504)

HH           7       2169729.0      1668.90      821.433       5.5073511       59.050312
17.230092       8.8177222       131.64553       311.64553           6

HH           5       1404225.0      1989.22      1087.66       5.5659565       59.085843
12.712738       6.2459298       88.832837       268.83284           4

HH (HV)           9 (7)       49154120. (6095961.0)      1707.56 (1710.69)      1382.69
(1377.64)       5.4940614 (5.4949263)       59.113053 (59.112560)       12.441768
(11.254518)       7.6377671 (6.2319136)       80.739896 (92.906109)       260.73990
(272.90611)         506 (505)

HH           7       1646089.0      1699.00      1386.51       5.4920649       59.113331
26.134262       5.4568279       353.15254       173.15254          14

HH          13       1679616.0      2697.89      1737.29       5.6936579       59.171259
29.448388       10.522076       13.545901       193.54590          17

HH (HV)          17 (17)       29986576. (1110916.0)      2406.85 (2406.38)      2098.77
(2100.81)       5.6172092 (5.6170308)       59.205582 (59.205794)       31.463601
(26.114536)       9.2779909 (12.625643)       352.73309 (341.18135)       172.73309
(161.18135)         526 (516)

HH           7       20948928.      2406.84      2104.14       5.6169770       59.206245
25.042226       7.7346906       8.1201479       188.12015          10

HH           6       614656.00      4098.44      3197.34       5.9412001       59.359492
14.148124       7.9357519       340.03837       160.03837           5

HH (HV)           6 (6)       1476225.0 (458329.00)      875.484 (875.914)      4407.49
(4406.52)       5.1960387 (5.1961716)       59.431355 (59.431253)       338.17432
(344.36144)       307.29445 (331.00006)       132.58114 (315.63138)       312.58114
(135.63138)         509 (509)
```

Table 3.1 Report with alarms produced by the ship detector, for an ASAR AP HH/HV image acquired 31-JAN-2008.

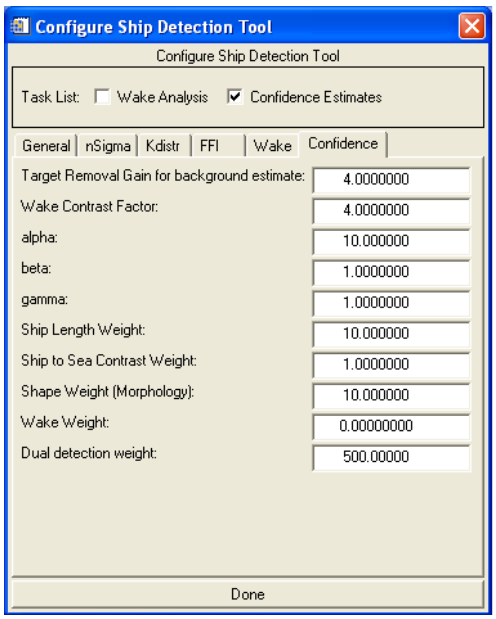

Figure 3.8 GUI for configuring the confidence estimation. The "Dual detection weight" is included to let the user set a value that will be added to the estimated confidence if a target is detected in more than one polarisation channel.

4 Experimental Results

The thresholding algorithms described in section 3 are implemented, and have so far been tested on a number of ENVISAT ASAR AP images.

In this study, the N-sigma algorithm was run with the parameter $N = 15$, and for the K-distribution algorithm the parameter $CFAR = 10^{-7}$. v was estimated based on equation (3.5).

The images were acquired from the Vestfjord in Northern Norway, Boknafjord in South-Western Norway and the Trondheimsfjord areas. These are areas with significant ship traffic and a variety of vessels: Fishing vessels, ferries and coastal freighters.

All images were processed and delivered by KSAT. AIS data logs are applied as "ground truth" for performance evaluation of the algorithms (see Appendix B for a description of the data material).

The positions reported by the automatic ship detector in Aegir and the positions from the AIS reports were all converted to shape-files (.shp) and overlaid the SAR image in ERDAS for the purpose of comparison. Examples are given in Figure 4.1 and Figure 4.2.

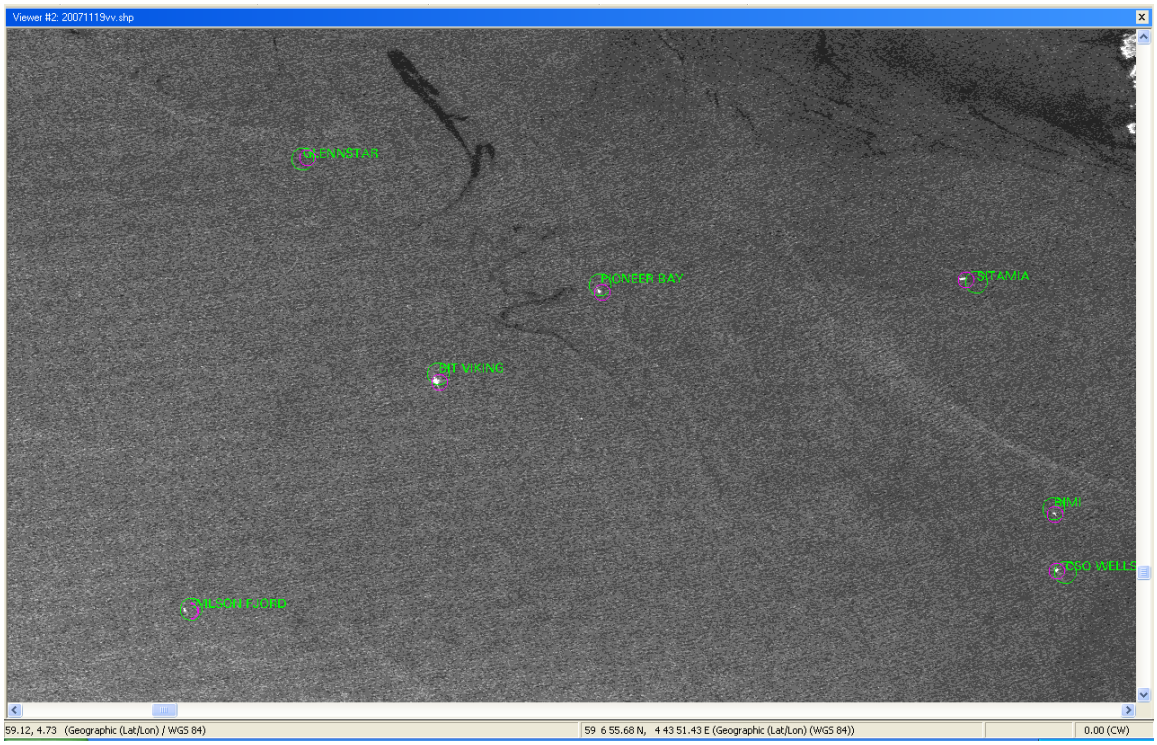

Figure 4.1 ENVISAT AP Image, 19th of November 2007 VV. Detected ships (purple, K-dist). AIS reports (green).

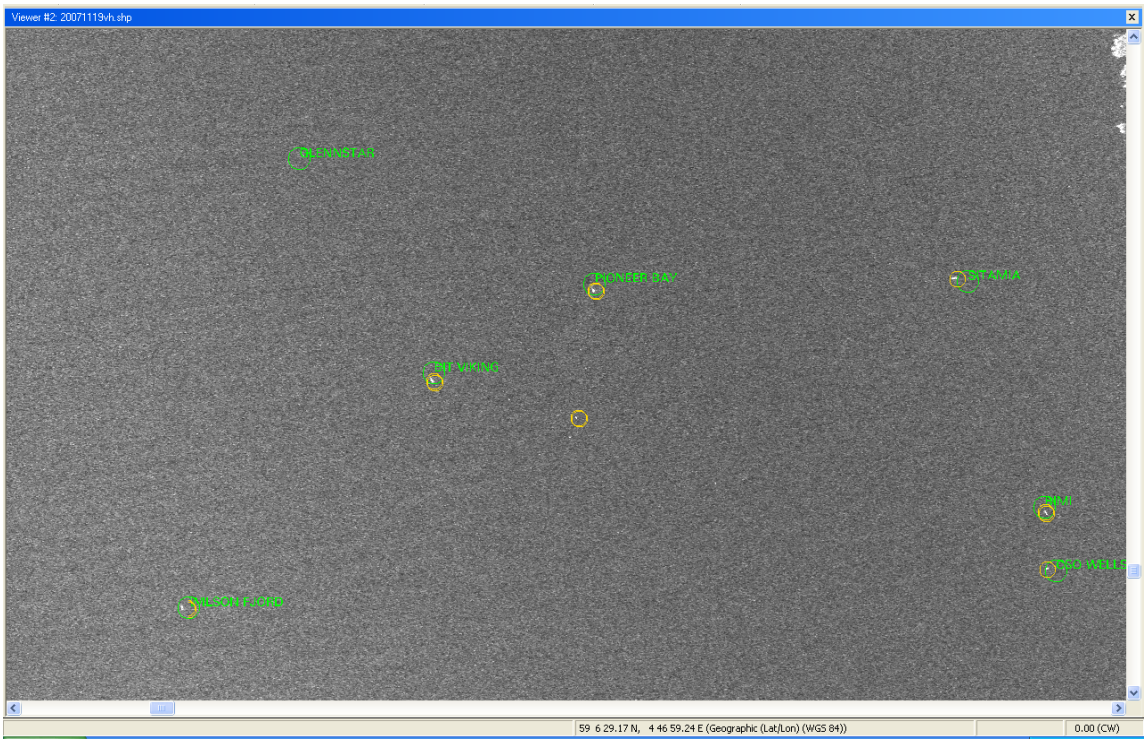

Figure 4.2 ENVISAT AP Image, 19th of November 2007 VH + detected ships (yellow, K-dist). AIS reports (green).

4.1 N-sigma on cross-pol channels (VH or HV)

The results from running the N-sigma algorithm on the cross-polarised bands are presented in Table 4.1 and Table 4.2.

Scene	Number of alarms
26.10.2007 20:30:58	9
14.12.2007 10:00:15	16
29.11.2007 21:01:07	10
20.12.2007 20:03:16	2
27.1.2008 20:09:01	10
30.01.2008 20:14:46	19
19.11.2007 21:15:26	20
08.12.2007 09:48:59	1
10.12.2007 20:17:37	11
25.10.2007 21:02:22	4
26.10.2007 20:31:58	7
31.1.2008 21:21:14	5
16.12.2007 20:29:07	3
06.11.2007 21:24:00	4
Total alarms	**121**

Table 4.1 The number of alarms (on all images in the test set) reported by the automatic detection algorithm N-sigma on cross-polarised channels.

Scene		
27.1.2008 20:09:01	Number of alarms	10
	Verified by AIS	6 alarms (6 vessels)
	Not verified by AIS	4 alarms
30.01.2008 20:14:46	Number of alarms	19
	Verified by AIS	3 alarms (3 vessels)
	Not verified by AIS	16 alarms
19.11.2007 21:15:26	Number of alarms	20
	Verified by AIS	17 alarms (12 vessels)
	Not verified by AIS	3 alarms
08.12.2007 09:48:59	Number of alarms	1
	Verified by AIS	1 alarm (1 vessel)
	Not verified by AIS	0 alarms
31.1.2008 21:21:14	Number of alarms	5
	Verified by AIS	3 alarms (3 vessels)
	Not verified by AIS	2 alarms
06.11.2007 21:24:00	Number of alarms	4
	Verified by AIS	2 alarms (2 vessels)
	Not verified by AIS	2 alarms

Scene	
Total alarms	**59**
Total verified	**32 alarms (27 vessels)**
Total not verified	**27 alarms**

Table 4.2 The number of alarms verified by AIS reports on a selected number of cross-polarised images.

4.2 N-sigma on co-pol channels (VV or HH)

The results from running the N-sigma algorithm on the co-polarised bands are presented in Table 4.3 and Table 4.4.

Scene	Number of alarms
26.10.2007 20:30:58	6
14.12.2007 10:00:15	0
29.11.2007 21:01:07	2
20.12.2007 20:03:16	0
27.1.2008 20:09:01	1
30.01.2008 20:14:46	13
19.11.2007 21:15:26	27
08.12.2007 09:48:59	5
10.12.2007 20:17:37	14
25.10.2007 21:02:22	38
26.10.2007 20:31:58	24
31.1.2008 21:21:14	11
16.12.2007 20:29:07	2
06.11.2007 21:24:00	6
Total alarms	**149**

Table 4.3 The number of alarms (on all images in the test set) reported by the automatic detection algorithm N-sigma on co-polarised channels.

Scene		
27.1.2008 20:09:01	Number of alarms	1
	Verified by AIS	0 alarms (0 vessels)
	Not verified by AIS	1 alarm
30.01.2008 20:14:46	Number of alarms	13
	Verified by AIS	2 alarms (2 vessels)
	Not verified by AIS	11 alarms

Scene		
19.11.2007 21:15:26	Number of alarms	27
	Verified by AIS	20 alarms (17 vessels)
	Not verified by AIS	7 alarms
08.12.2007 09:48:59	Number of alarms	5
	Verified by AIS	2 alarms (2 vessels)
	Not verified by AIS	3 alarms
31.1.2008 21:21:14	Number of alarms	11
	Verified by AIS	5 alarms (3 vessels)
	Not verified by AIS	6 alarms
06.11.2007 21:24:00	Number of alarms	6
	Verified by AIS	2 alarms (2 vessels)
	Not verified by AIS	4 alarms
Total alarms		**63**
Total verified		**31 alarms (26 vessels)**
Total not verified		**32 alarms**

Table 4.4 The number of alarms verified by AIS reports on a selected number of co-polarised images.

4.3 K-distribution on cross-polarised channels (VH or HV)

The results from running the K-distribution algorithm on the cross-polarised bands are presented in Table 4.5 and Table 4.6.

Scene	Number of alarms
26.10.2007 20:30:58	8
14.12.2007 10:00:15	9
29.11.2007 21:01:07	11
20.12.2007 20:03:16	0
27.1.2008 20:09:01	4
30.01.2008 20:14:46	4
19.11.2007 21:15:26	26
08.12.2007 09:48:59	0
10.12.2007 20:17:38	1
25.10.2007 21:02:22	2
26.10.2007 20:31:58	5
31.1.2008 21:21:14	3
16.12.2007 20:29:07	0
06.11.2007 21:24:00	2

Total alarms	**75**

Table 4.5 The number of alarms (on all images in the test set) reported by the automatic detection algorith K-distribution on cross-polarised channels.

Scene		
27.1.2008 20:09:01	Number of alarms	4
	Verified by AIS	4 alarms (3 vessels)
	Not verified by AIS	0 alarms
30.01.2008 20:14:46	Number of alarms	4
	Verified by AIS	2 alarms (2 vessels)
	Not verified by AIS	2 alarms
19.11.2007 21:15:26	Number of alarms	26
	Verified by AIS	23 alarms (13 vessels)
	Not verified by AIS	3 alarms
08.12.2007 09:48:59	Number of alarms	0
	Verified by AIS	0 alarms (0 vessels)
	Not verified by AIS	0 alarms
31.1.2008 21:21:14	Number of alarms	3
	Verified by AIS	2 alarms (2 vessels)
	Not verified by AIS	1 alarm
06.11.2007 21:24:00	Number of alarms	2
	Verified by AIS	2 alarms (2 vessels)
	Not verified by AIS	0 alarms
Total alarms		**39**
Total verified		**33 alarms (22 vessels)**
Total not verified		**6 alarms**

Table 4.6 The number of alarms verified by AIS reports on a selected number of cross-polarised images.

4.4 K-distribution on co-polarised channels (VV or HH)

The results from running the K-distribution algorithm on the co-polarised bands are presented in Table 4.7 and Table 4.8.

Scene	Number of alarms
26.10.2007 20:30:58	30
14.12.2007 10:00:15	0
29.11.2007 21:01:07	2
20.12.2007 20:03:16	0
27.1.2008 20:09:01	0
30.01.2008 20:14:46	1
19.11.2007 21:15:26	33
08.12.2007 09:48:59	6
10.12.2007 20:17:38	4
25.10.2007 21:02:22	62
26.10.2007 20:31:58	16
31.1.2008 21:21:14	3
16.12.2007 20:29:07	0
06.11.2007 21:24:00	1
Total alarms	**158**

Table 4.7 The number of alarms (on all images in the test set) reported by the automatic detection algorithm K-distribution on co-polarised channels.

Scene		
27.1.2008 20:09:01	Number of alarms	0
	Verified by AIS	0 alarms (0 vessels)
	Not verified by AIS	0 alarms
30.01.2008 20:14:46	Number of alarms	1
	Verified by AIS	1 alarm (1 vessel)
	Not verified by AIS	0 alarms
19.11.2007 21:15:26	Number of alarms	33
	Verified by AIS	28 alarms (16 vessels)
	Not verified by AIS	5 alarms
08.12.2007 09:48:59	Number of alarms	6
	Verified by AIS	3 alarms (3 vessels)
	Not verified by AIS	3 alarms
31.1.2008 21:21:14	Number of alarms	3
	Verified by AIS	2 alarms (2 vessels)
	Not verified by AIS	1 alarm
06.11.2007 21:24:00	Number of alarms	1
	Verified by AIS	1 alarm (1 vessel)
	Not verified by AIS	0 alarm

Total alarms		**44**
Total verified		**35 alarms (23 vessels)**
Total not verified		**9 alarms**

Table 4.8 The number of alarms verified by AIS reports on a selected number of co-polarised images.

5 Summary and Future Work

The total number of alarms on the total number of 14 SAR images in the test set is larger for the co-polarised bands than for cross-polarised bands; both for the N-sigma algorithm and the K-distribution algorithm (see Table 4.1, Table 4.3, Table 4.5 and Table 4.7). For the N-sigma algorithm 121 alarms were reported by the system on the cross-polarised bands, and 149 alarms were reported on the co-polarised bands. For the K-distribution algorithm 75 alarms were reported on the cross-polarised bands and as many as 158 alarms were reported on the co-polarised bands. For the cross-polarised bands, the total number of alarms is larger for the N-sigma algorithm. While for the co-polarised bands, the total number of alarms is larger for the K-distribution algorithm.

The results from the automatic ship detection algorithms on 6 out of the 14 SAR images in the test set were compared with AIS reports. The results for the N-sigma algorithm are presented in Table 4.2 and Table 4.4. For the N-sigma algorithm, we found a higher false alarm ratio for co-polarised bands (32/63 alarms) than for cross-polarised bands (27/59 alarms). A slightly higher number of verified ships were also detected in cross-polarisation (27 AIS reported ships) compared to co-polarisation (26 AIS reported ships). In summary, this gives us an indication that the N-sigma algorithm performes better on cross-polarised bands (VH or HV) than co-polarised bands (VV or HH), both in terms of successful detections and false alarms.

The N-sigma algorithm was compared to the K-distribution algorithm. The results for the K-distribution algorithm are presented in Table 4.6 and Table 4.8. For the K-distribution algorithm, we also here found a slightly higher false alarm ratio for co-polarised bands (9/44 alarms) than for cross-polarised bands (6/39 alarms), but for co-polarised bands a slightly higher number of verified ships were detected (23 AIS reported ships) than for cross-polarised bands (22 AIS reported ships). Comparing the results from the N-sigma algorithm and the K-distribution algorithm, we have found that the K-distribution algorithm produces a significant lower false alarm ratio for both cross-polarisation and co-polarisation. However the successful detection rate is lower when running the K-distribution algorithm compared to the N-sigma algorithm, both for cross-polarisation and co-polarisation.

Co-polarised bands (VV and HH) are expected to be sensitive to increasing wind speed, which might lead to false detections in rough sea. An increased ship/sea clutter contrast is expected for cross-polarised bands (VH and HV). Therefore it might not be a surprise that the number of false

alarms is higher for co-polarisation than cross-polarisation. However, it might not be correct to call the unverified alarms “false”. The “false” alarms might be vessels without the AIS turned on. It could also be a significant time difference between the AIS report sent by a particular vessel and the SAR acquisition. A more detailed investigation of the AIS reports, then what is done here, so far, might give some answers.

Future work should include running the algorithms on the same data set but with various parameter settings. A larger test data set should also be included to be able to produce even more reliable statistics. A very important issue is also to look into the reasons for the false alarms; are they real false alarms caused by other phenomena/objects than vessels due to e.g. bad landmasks, are they ships without the AIS turned on or is it simply a time difference between the AIS report and the SAR acquisition causing an uncorrelation between the positions?

As the signal return from the sea in cross-polarised bands are dominated by noise rather than sea clutter, the K-distribution might not be optimal as a model for the cross-polarised channels. Other distributions should be looked into. It would also be interesting to compare the algorithms with other detection approaches proposed in the literature. It might be a good idea to apply different models or algorithms depending on the polarisation channel.

References

[1] International Maritime Organization (2004): International Convention for the Safety of Life at Sea (SOLAS). Originally published 1974.

[2] Arnesen and Olsen (2004): ”Vurdering av ENVISAT ASAR for skipsdeteksjon”, FFI/Rapport-2004/02121

[3] Arnesen and Olsen (2004): ”Literature Review on Vessel Detection”, FFI/Rapport-2004/02619

[4] ASAR Product Handbook: http://envisat.esa.int/dataproducts/asar/

[5] Attema (2005), “Mission Requirements Document for the European Radar Observatory Sentinel-1”, Requirement Specification, European Space Agency, ES-RS-ESA-SY-0007, issue 1, revision 4, 2005

[6] Brekke et al. (2008), ”Ship traffic monitoring using multi-polarisation satellite SAR images combined with AIS reports”, In proceedings of EUSAR 2008, Friedrichshafen, Germany, 4 pages.

[7] Eldhuset (1996), “An Automatic Ship and Ship Wake Detection System for Spaceborne SAR Images in Coastal Regions”, IEEE Trans. on Geoscience and Remote Sensing, vol. 34, No. 4, July 1996, pp. 1010-1019

[8] Johnsen and Larsen (2006), “A Novel Method for Spaceborne SAR Vessel detection Using Complex Radar Backscatter”, Work Package Report Wp-1100 and Wp-2100 Norut Informasjonsteknologi AS, ESTEC/Contract No: 18995/05/NL/MV, European Space Agency

[9] Oliver and Quegan (1998): “Understanding Synthetic Aperture Radar Images”, Artech House, Inc.

[10] Redding (1999), “Estimating the Parameters of the K Distribution in the Intensity Domain”, Surveillance Systems Division, Electronics and Surveillance Research Laboratory, DSTO-TR-0839, Department of Defence, Australia

[11] Rey et al. (1996): “A search procedure for ships in RADARSAT imagery (U)”, Defense Research Establishment Ottawa, Report No. 1305

[12] Weydahl et al. (2007), “Ship traffic monitoring using satellite SAR images in combination with AIS reports”, In proceedings of SPIE 2007, Firence, Italy, vol. 6749, 7 pages.

[13] RADAR and SAR Glossary: http://envisat.esa.int/handbooks/asar/CNTR5-2.htm

Abbreviations

AIS	Automatic Identification System
AP	Alternating Polarisation
ASAR	Advanced Synthetic Aperture Radar
CFAR	Constant False Alarm Rate
EMSA	European Maritime Safety Agency
ENL	Equivalent Number of Looks
GUI	Graphical User Interface
IHP	Internal Hermittian Product
IMO	International Maritime Organization
KSAT	Kongsberg Satellite Services
LIMES	Land and Sea Integrated Monitoring for Environment and Security
PDF	Probability Density Function
SAR	Synthetic Aperture Radar
TCR	Target-to-Clutter Ratio

Appendix A K-distribution algorithm: look-up tables

A.1 CFAR: 0.0000001

ENL	*v*	*t*
1.0	5.0	32.3372530103729330
	10.0	25.0723580041031010
	15.0	22.3991160013551250
	20.0	20.9821949998985920
	40.0	18.7055519975583020
	90.0	-
2.0	5.0	20.2619339991581950
	10.0	15.4860609951617470
	15.0	13.7276789964777210
	20.0	12.7942589971762930
	40.0	11.2895769983023970
	90.0	10.3695259989909640
3.0	5.0	15.9102209948443050
	10.0	12.0443629977375150
	15.0	10.6203179988032710
	20.0	9.8635499993696367
	40.0	8.6407550002847771
	90.0	7.8893780007488568
4.0	5.0	13.6166519965608130
	10.0	10.2336029990926890
	15.0	8.9868610000257512
	20.0	8.3237330005220365
	40.0	7.2502150006595159
	90.0	6.5879140005669408

A.2 CFAR: 0.00000001

ENL	*v*	*t*
1.0	5.0	-
	10.0	-
	15.0	20.0000019988889410
	20.0	20.0000019988889410
	40.0	20.0000019988889410
	90.0	-
2.0	5.0	-
	10.0	18.3243529971664460
	15.0	16.0869139948664570
	20.0	14.8998299956004820
	40.0	12.9846719970337880
	90.0	11.8094659979133120
3.0	5.0	18.9816659978421360
	10.0	14.1167729961865230
	15.0	12.3304539975234050
	20.0	11.3819769982332450
	40.0	9.8488249993806569
	90.0	8.9039850000877756
4.0	5.0	16.1272319949079020
	10.0	11.9117899978367330
	15.0	10.3636999989953240
	20.0	9.5411879996108926
	40.0	8.2095870006074634
	90.0	7.3860650006785047

Appendix B Data Set

B.1 ENVISAT AP data

ENVISAT ASAR AP images from both “Ascending” and “Descending” passes are applied in this study. However, mainly “Ascending” passes are selected to avoid conflicting orders. ENVISAT ASAR AP products contain two co-registered images corresponding to one of the three polarisation combination submodes: HH/VV, HH/HV or VV/VH. The images acquired in this study have a polarisation combination of VV/VH or HH/HV. The specifications for ASAR AP Precision images are [4]: pixel spacing (range x azimuth) of 12.5 m x 12.5 m, nominal resolution of (range x azimuth) 30 m x 30 m and approximate coverage of (range x azimuth) 56-100 km x 100 km. See Table 1 for an overview of the scenes.

Date and time (UTC)	**Ascending/ Descending**	**Beam**	**Polari-sation**	**Scene**	**AIS data available**
26.10.2007 20:30:58	A	IS1	VV/VH	Trondheim	Log not decoded yet
14.12.2007 10:00:15	A	IS2	VV/VH	Vestfjorden	10:10 UTC
29.11.2007 21:01:07	A	IS2	VV/VH	Boknafjorden	20:45 UTC
20.12.2007 20:03:16	A	IS2	HH/HV	Vestfjorden	20:10 UTC
27.1.2008 20:09:01	A	IS2	HH/HV	Vestfjorden	20:09 UTC
30.01.2008 20:14:46	A	IS3	HH/HV	Vestfjorden	20:15 UTC
19.11.2007 21:15:26	A	IS4	VV/VH	Boknafjorden	21:15 UTC
08.12.2007 09:48:59	D	IS4	VV/VH	Vestfjorden	09:48 UTC
10.12.2007 20:17:38	A	IS4	VV/VH	Vestfjorden	20:10 UTC
25.10.2007 21:02:22	A	IS6	VV/VH	Trondheim	Log not decoded yet
26.10.2007 20:31:58	A	IS6	HH/HV	Vestfjorden	Log not decoded yet
31.1.2008 21:21:14	A	IS6	HH/HV	Boknafjorden	21:21 UTC
16.12.2007 20:29:07	A	IS6	VV/VH	Vestfjorden	-
06.11.2007 21:24:00	A	IS7	VV/VH	Boknafjorden	21:24 UTC

Table 1 ENVISAT ASAR AP scenes applied in this study.

ENVISAT ASAR AP images can be acquired with the various beams described in Table 2.

Beam	Incidence angle [°]
IS1	15.0—22.9
IS2	19.2—26.7
IS3	26.0—31.4
IS4	31.0—36.3
IS5	35.8—39.4
IS6	39.1—42.8
IS7	42.5—45.2

Table 2 ENVISAT ASAR AP beams.

B.2 AIS Data Logs

The Norwegian Coastal Administration is the Norwegian national agency for coastal management, marine safety and communication. The Norwegian Coastal Administration has deployed base stations for reception of AIS data along the Norwegian coast. See Figure 1. Other national agencies in Europe have done the same.

AIS data are available from the web-site http://ais2.aisonline.com/aisnmd/ provided by the Norwegian Coastal Administration. A username and a password are needed for access.

In this study, we downloaded AIS data from the web-site and used it as “ground truth” during performance testing.

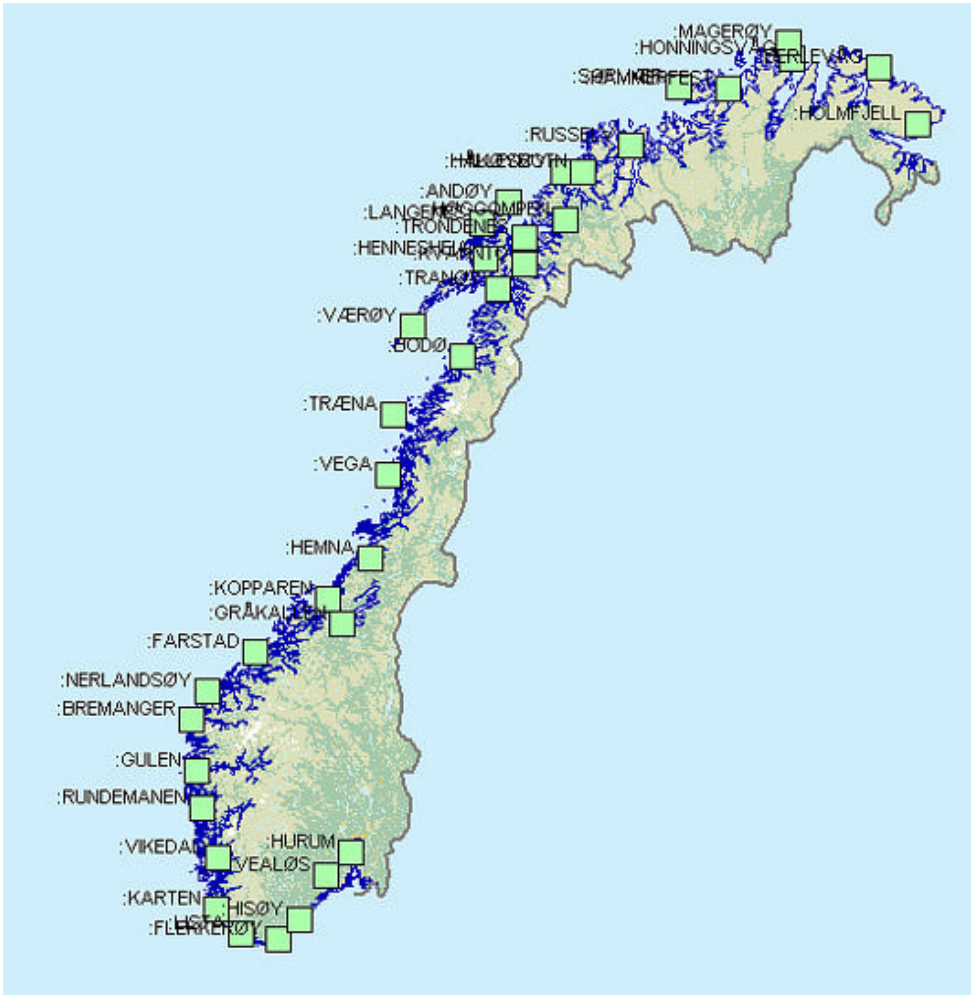

Figure 1 Locations of AIS base stations along the Norwegian coast.

Appendix C Ship Detection Report Standard

```
<?xml version="1.0" encoding="utf-8" ?>
- <!--
edited with XMLSpy v2006 sp2 U (http://www.altova.com) by Gudmundur Jokulsson (KSAT)
-->
<xsd:schema xmlns:xsd="http://www.w3.org/2001/XMLSchema"
xmlns:gml="http://www.opengis.net/gml"
xmlns:wfsvd="http://cweb.ksat.no/cweb/schema/geoweb/vessel"
targetNamespace="http://cweb.ksat.no/cweb/schema/geoweb/vessel"
elementFormDefault="qualified" attributeFormDefault="unqualified" version="3.1.1" id="wfsvd">
<xsd:annotation>
<xsd:documentation>Copyright (c) 2006 KSAT, All Rights Reserved. Satellite based Vessel
Detection - GML Application schema</xsd:documentation>
</xsd:annotation>
- <!--
======================================================================
-->
- <!--
GML IMPORT
-->
<xsd:import namespace="http://www.opengis.net/gml"
schemaLocation="http://schemas.opengis.net/gml/3.1.1/base/feature.xsd" />
- <!--
============================================================
-->
- <!--
globally defined wfsvd: elements (direct from gml or xsd namespace types)
-->
<xsd:element name="vesselPosition" type="gml:PointPropertyType"
substitutionGroup="gml:pointProperty">
<xsd:annotation>
<xsd:documentation>The point position of a vessel</xsd:documentation>
</xsd:annotation>
</xsd:element>
<xsd:element name="vesselLength" type="xsd:decimal">
<xsd:annotation>
<xsd:documentation>In meters</xsd:documentation>
</xsd:annotation>
</xsd:element>
<xsd:element name="vesselBeam" type="xsd:decimal">
<xsd:annotation>
<xsd:documentation>In meters</xsd:documentation>
</xsd:annotation>
</xsd:element>
<xsd:element name="vesselHeading" type="xsd:decimal">
<xsd:annotation>
<xsd:documentation>In decimal deegrees of angle</xsd:documentation>
</xsd:annotation>
</xsd:element>
<xsd:element name="vesselSpeedOverGround" type="xsd:decimal">
<xsd:annotation>
<xsd:documentation>In knots</xsd:documentation>
</xsd:annotation>
</xsd:element>
```

```
<xsd:element name="vesselType" type="xsd:string">
<xsd:annotation>
<xsd:documentation>Type of vessel detected.</xsd:documentation>
</xsd:annotation>
</xsd:element>
<xsd:element name="vesselProbability" type="xsd:integer">
<xsd:annotation>
<xsd:documentation>Probability of correctness of oberservation (range 0 to 100)</xsd:documentation>
</xsd:annotation>
</xsd:element>
<xsd:element name="productID" type="xsd:string">
<xsd:annotation>
<xsd:documentation>Satellite product ID - unique identification of a product</xsd:documentation>
</xsd:annotation>
</xsd:element>
<xsd:element name="startTime" type="xsd:dateTime">
<xsd:annotation>
<xsd:documentation>Start time of product scene</xsd:documentation>
</xsd:annotation>
</xsd:element>
<xsd:element name="stopTime" type="xsd:dateTime">
<xsd:annotation>
<xsd:documentation>Stop time of product scene</xsd:documentation>
</xsd:annotation>
</xsd:element>
- <!--
=====================================================================
-->
- <!—
VD Feature Type
-->
<xsd:element name="feature" type="wfsvd:FeatureType" substitutionGroup="gml:_Feature">
<xsd:annotation>
<xsd:documentation>An VD feature encloses a snapshot of a single detected
vessel</xsd:documentation>
</xsd:annotation>
</xsd:element>
<xsd:complexType name="FeatureType">
<xsd:complexContent>
<xsd:extension base="gml:AbstractFeatureType">
<xsd:sequence>
<xsd:annotation>
<xsd:documentation>The actual detected vessel feature</xsd:documentation>
</xsd:annotation>
<xsd:element ref="wfsvd:vesselPosition" />
<xsd:element ref="wfsvd:vesselType" minOccurs="0" />
<xsd:element ref="wfsvd:vesselLength" minOccurs="0" />
<xsd:element ref="wfsvd:vesselBeam" minOccurs="0" />
<xsd:element ref="wfsvd:vesselSpeedOverGround" minOccurs="0" />
<xsd:element ref="wfsvd:vesselHeading" minOccurs="0" />
<xsd:element ref="wfsvd:vesselProbability" minOccurs="0" />
<xsd:element ref="wfsvd:productID" minOccurs="0" />
  <xsd:element ref="wfsvd:startTime" minOccurs="0" />
  <xsd:element ref="wfsvd:stopTime" minOccurs="0" />
  <xsd:element name="provider" type="xsd:string" minOccurs="0" />
```

```
<xsd:element name="access" type="xsd:string" minOccurs="0" />
</xsd:sequence>
</xsd:extension>
</xsd:complexContent>
</xsd:complexType>
- <!--
 ======================================================
 -->
 - <!--
 ================================================
 -->
 - <!--
 ================================================
 -->
<xsd:element name="featureMember" type="wfsvd:FeaturePropertyType"
substitutionGroup="gml:featureMember" />
- <!--
 ============================================================
 -->
<xsd:complexType name="FeaturePropertyType">
 <xsd:annotation>
<xsd:documentation>Restricted feature property Container for a wfsvd:feature – follow
gml:AssociationType pattern.</xsd:documentation>
 </xsd:annotation>
<xsd:complexContent>
<xsd:restriction base="gml:FeaturePropertyType">
<xsd:sequence minOccurs="0">
<xsd:element ref="wfsvd:feature" />
 </xsd:sequence>
<xsd:attributeGroup ref="gml:AssociationAttributeGroup" />
 </xsd:restriction>
 </xsd:complexContent>
 </xsd:complexType>
- <!--
 ============================================================
 -->
<xsd:element name="featureCollection" type="wfsvd:FeatureCollectionType"
substitutionGroup="gml:_FeatureCollection">
<xsd:annotation>
<xsd:documentation>This is the concrete response element used by a service for VD
features</xsd:documentation>
 </xsd:annotation>
 </xsd:element>
<xsd:complexType name="FeatureCollectionType">
 <xsd:annotation>
<xsd:documentation>A restriction of the abstract feature collection contains zero or more
wfsvd:featureMembers.</xsd:documentation>
 </xsd:annotation>
<xsd:complexContent>
 <xsd:restriction base="gml:AbstractFeatureCollectionType">
<xsd:sequence>
<xsd:group ref="gml:StandardObjectProperties" />
<xsd:element ref="gml:boundedBy" minOccurs="0" />
<xsd:element ref="wfsvd:featureMember" minOccurs="0" maxOccurs="unbounded" />
</xsd:sequence>
<xsd:attribute ref="gml:id" use="optional" />
</xsd:restriction>
</xsd:complexContent>
```

```
</xsd:complexType>
</xsd:schema>
```